



Thermal behaviour of mandelic acid, sodium mandelate and its compounds with some bivalent transition metal ions

D.J.C. Gomes, F.J. Caires*, L.S. Lima, A.C. Gigante, M. Ionashiro

Instituto de Química, Universidade Estadual Paulista, CP 355, 14801-970 Araraquara, SP, Brazil

ARTICLE INFO

Article history:

Received 24 October 2011

Received in revised form 8 December 2011

Accepted 11 January 2012

Available online 25 January 2012

Keywords:

Bivalent transition metals

Mandelate

Thermal decomposition

TG–FTIR

Evolved gases

ABSTRACT

Characterization, thermal stability and thermal decomposition of transition metal mandelates, $M(C_6H_5CH(OH)CO_2)_2$ ($M = Mn(II), Fe(II), Co(II), Ni(II), Cu(II), Zn(II)$), as well as the thermal behaviour of mandelic acid $C_6H_5CH(OH)CO_2H$ and its sodium salt were investigated employing simultaneous thermogravimetry and differential scanning calorimetry (TG–DSC), TG–DSC coupled to FTIR, infrared spectroscopy (FTIR), elemental analysis and complexometry. All the compounds were obtained in the anhydrous state and the thermal decomposition occurs in two or four consecutive steps. The final residue up to 320 °C (Mn), 345 °C (Fe), 400 °C (Co), 405 °C (Ni), 355 °C (Cu) and 575 °C (Zn) is $Mn_3O_4, Fe_2O_3, Co_3O_4, NiO, CuO$ and ZnO , respectively. The results also provided information concerning the ligand's denticity, thermal behaviour and identification of gaseous products evolved during the thermal decomposition of these compounds.

© 2012 Elsevier B.V. All rights reserved.

1. Introduction

Mandelic acid is an aromatic alpha hydroxy acid with the molecular formula $C_6H_5CH(OH)CO_2H$. It has a long history of use in medicine as an antibacterial, particularly in the treatment of urinary tract infections [1]. A survey of literature shows that the papers involving bivalent transition metal mandelates reported the structure studies on the glycolato, lactato and mandelato solid complexes of some bivalent iron series metal [2], infrared spectrum of nickel (II) mandelate complex [3], mixed-ligand complexes of copper (II) with α -hydroxycarboxylic acids and 1, 10-phenanthroline [4], syntheses, structures and magnetic properties of layered metal (II) mandelates [5] and mononuclear, dinuclear and hydroxo-bridged tetranuclear complexes from reactions of Cu (II) ions, mandelic acid diimine ligands [6]. However, few thermoanalytical studies with bivalent transition metal mandelates on solid state were found in the literature.

In this paper, the object of the present research was to investigate the thermal behaviour of mandelic acid and its sodium salt, as well as to prepare solid-state compounds of some bivalent transition metal ions (i.e. Mn(II), Fe(II), Co(II), Ni(II), Cu(II), Zn(II)) with mandelate and to characterize and to investigate by means of complexometry, elemental analysis, X-ray powder diffractometry, infrared spectroscopy (FTIR), simultaneous thermogravimetry and differential scanning calorimetry (TG–DSC) and TG–DSC coupled

to FTIR. The thermal studies were performed in dynamic air atmosphere.

2. Experimental

The mandelic acid, $C_6H_5CH(OH)CO_2H$ with 99% purity was obtained from Sigma and it was used as received. Aqueous solution of sodium mandelate 0.1 mol L^{-1} was prepared by neutralization of the aqueous solution of mandelic acid with 0.1 mol L^{-1} sodium hydroxide solution. Aqueous solutions of bivalent metal ions 0.1 mol L^{-1} were prepared by dissolving the corresponding chlorides (Mn(II), Co(II), Ni(II), Zn(II)) or sulphate (Fe(II), Cu(II)).

The solid-state compounds were obtained by adding 100.0 mL of sodium mandelate solution 0.1 mol L^{-1} to 50.0 mL of the respective metal ions solutions 0.1 mol L^{-1} . The resulting solutions were heated at ebullition with continuous stirring for about 1 h, and the precipitates were filtered off, washed with distilled water until chloride or sulphate ions were eliminated, dried at ambient temperature and kept in a desiccator over anhydrous calcium chloride. To avoid oxidation of Mn(II) and Fe(II), all the solutions, the water employed for washing the precipitate and the reactional system were purged with nitrogen gas. In the solid-state compounds, metal ions and mandelate contents were determined from TG curves. The metal ions were also determined by complexometry with standard EDTA solution after igniting the compounds to the respective oxides and their dissolution in hydrochloric acid solution [7,8].

Carbon and hydrogen contents were determined by calculations based on the mass losses of the TG curves, since the ligand lost

* Corresponding author. Tel.: +55 16 3301 9617.

E-mail address: caires.flavio@yahoo.com.br (F.J. Caires).

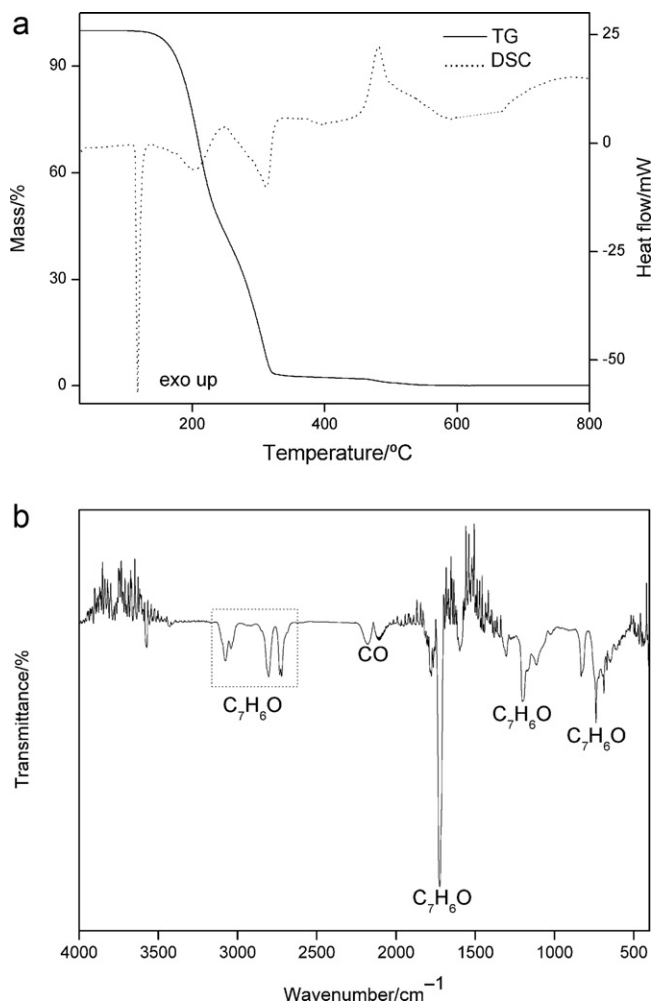


Fig. 1. (a) Simultaneous TG–DSC curves ($m = 11.7730$ mg) and (b) IR spectrum of the gases released during the thermal decomposition of mandelic acid.

during the thermal decomposition occurs with the formation of the respective oxides with stoichiometry known, as final residue.

X-ray powder patterns were obtained by using a Siemens D-5000 X-ray diffractometry, employing Cu K α radiation ($\lambda = 1.541$ Å) and a setting of 40 kV and 20 mA.

The attenuate total reflectance infrared spectra for mandelic acid and for its metal-ion compounds were run on a Nicolet iS10 FTIR spectrophotometer, using an ATR accessory with Ge window.

Simultaneous TG–DSC curves were obtained by using a TGA–DSC 1 Star^c system, from Mettler Toledo. The purge gas was an air flow of 50 mL min⁻¹ and a heating rate of 10 °C min⁻¹ was adopted, with samples weighing about 10 mg. Alumina crucibles were used for recording the TG–DSC curves.

The measurements of the gaseous products were carried out using a TG–DSC Mettler Toledo coupled to a FTIR spectrophotometer Nicolet with gas cell and DTGS KBr detector. The furnace and the heated gas cell (250 °C) were coupled through a heated ($T = 200$ °C) 120 cm stainless steel line transfer with diameter of 3 mm, both purged with dry air (50 mL min⁻¹). The FTIR spectra were recorded with 16 scans per spectrum at a resolution of 4 cm⁻¹.

3. Results and discussion

The TG–DSC curves and IR spectrum of the released products during the thermal decomposition of mandelic acid are shown in Fig. 1. The TG curve, Fig. 1(a), shows mass losses in three steps

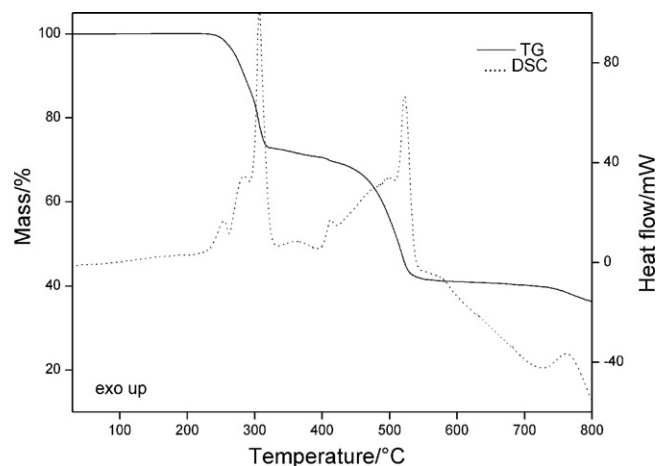


Fig. 2. Simultaneous TG–DSC curves of the sodium mandelate ($m = 10.1530$ mg).

between 125 and 230 °C, 230 and 330 °C and 330 and 550 °C and the corresponding DSC curve shows four thermal events. The first endothermic peak at 118 °C is due to the melting of mandelic acid and the endothermic peaks at 200 °C and 310 °C are attributed to the thermal decomposition of mandelic acid, which occurs in two steps with the formation of carbonaceous residue. The formation of carbonaceous residues was confirmed based on the TG–DSC curves of mandelic acid obtained up to 350 °C. The exothermic peak at 475 °C is attributed to the oxidation of the carbonaceous residue. The gaseous products evolved during the thermal decomposition were monitored and identified mostly on basis of their FTIR reference available on NICOLET libraries, as benzaldehyde and CO, as shown in Fig. 1(b).

For the anhydrous sodium mandelate the simultaneous TG–DSC curves, Fig. 2, show that the thermal decomposition occurs in two steps between 240 and 320 °C and 320 and 570 °C with losses of 26.99% and 31.62%, respectively corresponding to exothermic peaks at 255 °C, 285 °C, 310 °C and 520 °C attributed to the oxidation of the organic matter. The small thermal events observed between 350 and 450 °C are attributed to the initial thermal decomposition corresponding to the second mass loss. The total mass loss up to 580 °C is in disagreement with the formation of sodium carbonate (Calc. = 69.51%; TG = 58.60%), as observed in the thermal decomposition of sodium succinate and sodium malonate [9,10]. Tests with hydrochloric acid solution on sample heated up to the temperature indicated by the TG–DSC curves (580 °C) confirmed the formation of a black residue identified as a mixture of carbonaceous residue and sodium carbonate. The mass loss between 680 and 800 °C, corresponding to an exothermic peak at 770 °C is attributed to the oxidation of the carbonaceous residue.

The analytical and thermoanalytical (TG) data for the synthesized compounds are shown in Table 1. These results establish the stoichiometry of these compounds, which are in agreement with general formula: $M(L)_2$, where M represents Mn(II), Fe(II), Co(II), Ni(II), Cu(II) and Zn(II), and L is mandelate ($C_6H_5CH(OH)COO^-$).

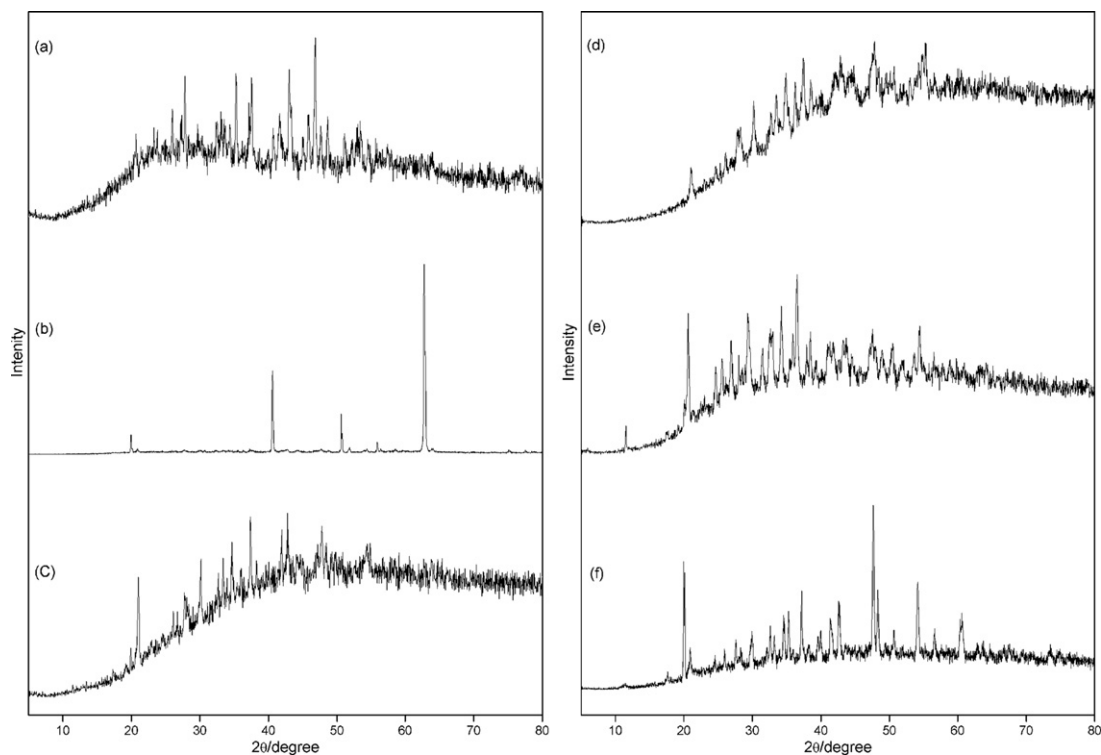
The X-ray diffraction powder patterns (Fig. 3) show that all the compounds have crystalline structure, without evidence for formation of isomorphous compounds and the crystallinity of these compounds follow the order: Fe > Zn > Mn \cong Cu > Co > Ni. The difference in the crystallinity of these compounds must be due to the velocity of precipitation, since the solid compounds are obtained heating the solution at ebullition temperature, and the heating, as well as the time of ebullition were not controlled.

The attenuate total reflectance spectroscopic data on mandelic acid and its compounds with the metal ions considered in this work

Table 1
Analytical and thermoanalytical (TG) data for the $M(C_6H_5CHOHCOO)_2$ compounds.

Compounds	Metal oxide (%)			L (lost) (%)		C (%)		H (%)		Final residue
	Calc.	EDTA	TG	Calc.	TG	Calc.	TG	Calc.	TG	
MnL ₂	21.35	21.64	22.10	78.65	77.90	53.78	53.27	3.96	3.92	Mn ₃ O ₄
FeL ₂	22.30	22.40	22.39	77.70	77.61	53.64	53.58	3.95	3.95	Fe ₂ O ₃
CoL ₂	22.22	22.63	22.28	77.78	77.72	53.18	53.14	3.91	3.90	Co ₃ O ₄
NiL ₂	20.69	20.23	20.73	79.31	79.27	53.22	53.19	3.92	3.92	NiO
CuL ₂	21.74	21.73	21.83	78.26	78.17	52.51	52.45	3.86	3.86	CuO
ZnL ₂	22.13	22.43	22.73	77.87	77.27	52.25	51.85	3.85	3.82	ZnO

L = mandelate.

**Fig. 3.** X-ray powder diffraction patterns of the compounds: (a) MnL₂, (b) FeL₂, (c) CoL₂, (d) NiL₂, (e) CuL₂ and (f) ZnL₂ (L = mandelate).

are shown in Table 2. These results show that in all the compounds $\nu_{as}(\text{COO}^-)$, $\nu(\text{O}-\text{H})$ and $\nu(\text{C}-\text{OH})$ are shifted toward lower energies than that observed in the free acid. This behaviour indicates that coordination is carried out through the hydroxyl and carboxyl groups [11], in agreement with Ref. [2].

Simultaneous TG–DSC curves of the compounds are shown in Fig. 4. These curves show mass losses in two or four steps, corresponding to endothermic and exothermic peaks attributed to thermal decomposition and oxidation of organic matter. These

curves also show that all the compounds were obtained in the anhydrous state.

The thermal stability of the compounds (I), as well as the final temperature of thermal decomposition (II) shown by TG–DSC curves depend on the nature of the metal ion, and they follow the order:

- (I) Zn > Ni > Co > Cu > Mn > Fe
 (II) Zn > Ni > Co > Cu > Fe > Mn

Table 2
Spectroscopic data for mandelic acid and its compounds with some bivalent transition metal ions.

Compounds	$\nu(\text{OH})$ (cm ⁻¹)	$\nu_{as}(\text{COO}^-)$ (cm ⁻¹)	$\nu_s(\text{COO}^-)$ (cm ⁻¹)	$\nu(\text{C}-\text{OH})$ (cm ⁻¹)
HL	3395 w,br	1711 s	–	1062 m
MnL ₂	3236 w,br	1563 s	1413 m	1018 m
FeL ₂	3249 w,br	1568 s	1417 m	1010 m
CoL ₂	3254 w,br	1571 s	1411 m	1001 m
NiL ₂	3246 w,br	1576 s	1412 m	999 m
CuL ₂	3139 w,br	1631 s	1350 m	997 m
ZnL ₂	3246 w,br	1592 s/1584 s	1336 m/1406 m	1008 m/1002 m

L = mandelate; w, br = weak, broad; s = strong; m = medium;

 $\nu(\text{OH})$ = hydroxyl oxygen–hydrogen stretching frequency; $\nu_{as}(\text{COO}^-)$ = antisymmetric carboxyl stretching frequency; $\nu_s(\text{COO}^-)$ = symmetric carboxyl stretching frequency; $\nu(\text{C}-\text{OH})$ = carbon–hydroxyl stretching frequency.

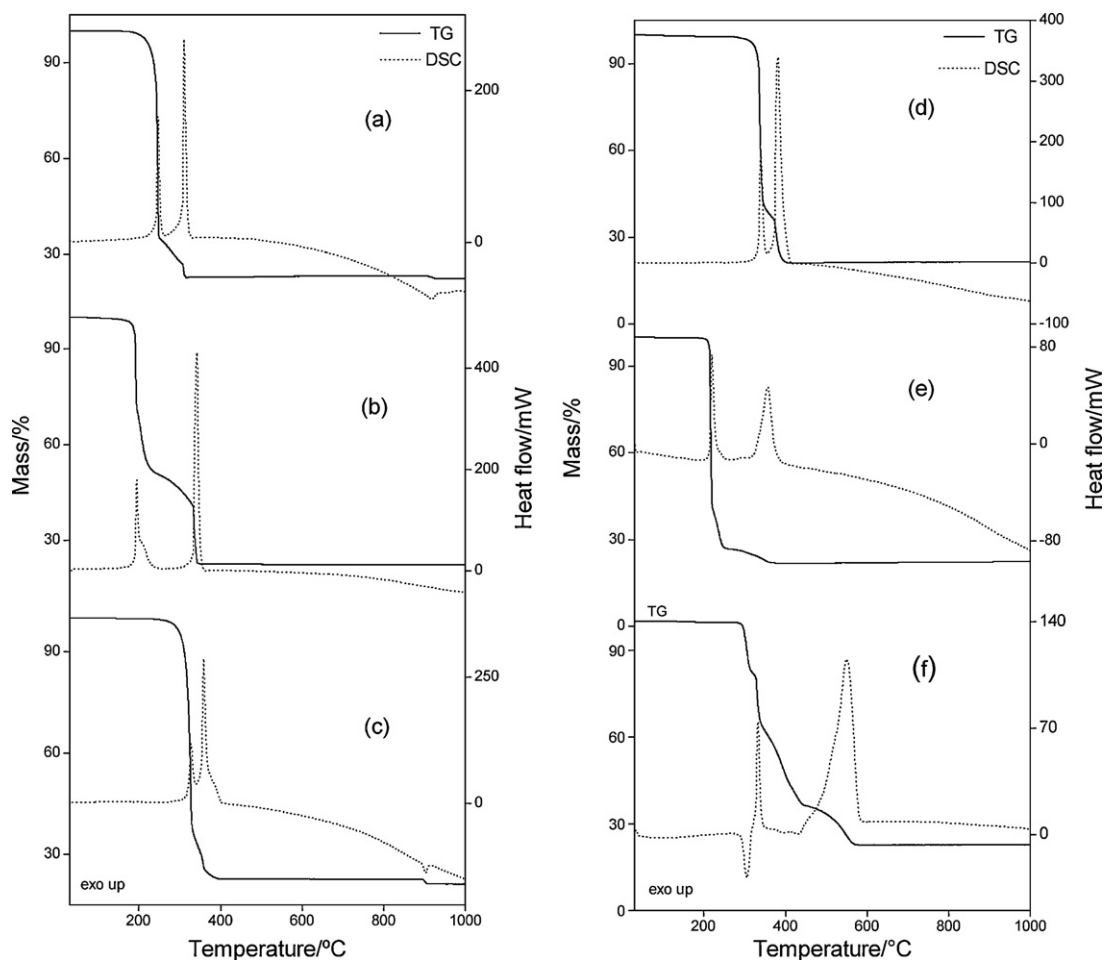


Fig. 4. Simultaneous TG–DSC curves of the compounds: (a) MnL_2 ($m = 10.060$ mg), (b) FeL_2 (10.019 mg), (c) CoL_2 (10.044 mg), (d) NiL_2 (10.089 mg), (e) CuL_2 (10.064 mg) and (f) ZnL_2 (10.045 mg).

The thermal behaviour of the compounds is also heavily dependent on the nature of the metal ion and so the features of each of these compounds are discussed individually.

3.1. Manganese compound

The simultaneous TG–DSC curves are shown in Fig. 4(a). The thermal decomposition of the anhydrous compound occurs in two steps, between 160 and 250 °C and 250 and 320 °C with losses of 65.21% and 12.69%, respectively corresponding to exothermic peak at 250 °C and 310 °C, which are attributed to oxidation of the organic matter. The total mass loss up to 320 °C is in agreement with the formation of Mn_3O_4 (Calc. = 78.65%; TG = 77.90%). The last mass loss observed between 900 and 930 °C, corresponding to an endothermic peak at 920 °C is attributed to the reduction of Mn_3O_4 to MnO in agreement with the literature [12].

3.2. Iron compound

The simultaneous TG–DSC curves are shown in Fig. 4(b). The thermal decomposition of the anhydrous compound occurs in four steps, between 80 and 195 °C, 195 and 230 °C, 230 and 330 °C and 330 and 345 °C, with losses of 29.32%, 18.40%, 17.79% and 12.10%, respectively corresponding to the exothermic peaks at 195 °C, 210 °C and 340 °C attributed to oxidation of Fe(II) to Fe(III) and organic matter. Absence of thermal events corresponding to the third mass loss suggests that in this step, endothermic and

exothermic reaction must be occurring simultaneously. The total mass loss up to 345 °C is in agreement with the formation of Fe_2O_3 , as final residue (Calc. = 77.70%; TG = 77.61).

3.3. Cobalt compound

The simultaneous TG–DSC curves are shown in Fig. 4(c). The thermal decomposition of the anhydrous compound occurs in two steps between 230 and 335 °C and 335 and 400 °C, with losses of 65.58% and 15.14% respectively corresponding to exothermic peaks at 330 °C and 335 °C attributed to oxidation of the organic matter. The total mass loss up to 400 °C is in agreement with the formation of Co_3O_4 (Calc. = 77.78%; TG = 77.72%). The last mass loss between 895 and 915 °C is attributed to reduction reaction of Co_3O_4 to CoO (Calc. = 1.48%; TG = 1.46%) [10,13].

3.4. Nickel compound

The simultaneous TG–DSC curves are shown in Fig. 4(d). The thermal decomposition of the anhydrous compound occurs in two steps between 270 and 350 °C and 350 and 405 °C with losses of 60.32% and 18.95%, respectively corresponding to exothermic peaks at 340 °C and 380 °C attributed to oxidation of the organic matter. The total mass loss up to 405 °C is in agreement with the formation of NiO , as final residue (Calc. = 79.31%; TG = 79.27%).

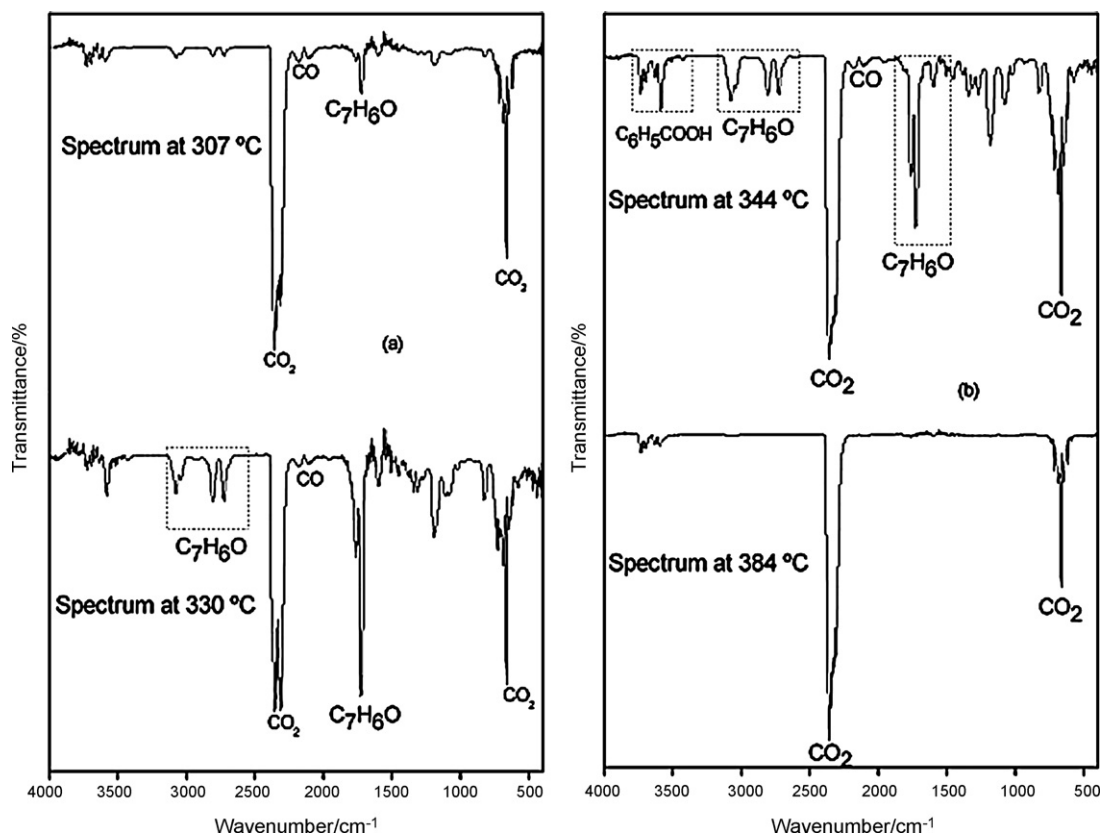


Fig. 5. IR spectra of gaseous products evolved during the decomposition of the compounds: (a) ZnL_2 (b) NiL_2 . L = mandelate.

3.5. Copper compound

The simultaneous TG–DSC curves are shown in Fig. 4(e). The thermal decomposition of the anhydrous compound also occurs in two steps between 180 and 250 °C and 250 and 365 °C with losses of 73.25% and 4.92%, respectively corresponding to exothermic peaks at 220 °C and 355 °C attributed to the oxidation of organic matter. The total mass loss up to 355 °C is in agreement with the formation of CuO , as final residue. (Calc. = 78.26%; TG = 78.17%.)

3.6. Zinc compound

The simultaneous TG–DSC curves are shown in Fig. 4(f). The thermal decomposition of the anhydrous compound occurs in four steps between 270 and 320 °C, 320 and 350 °C, 350 and 440 °C and 440 and 575 °C with losses of 17.74%, 17.74%, 24.47% and 17.32%, respectively corresponding to endothermic peak at 305 °C ascribed to the thermal decomposition and exothermic peaks at 330 °C and 545 °C attributed to the oxidation of the organic matter.

No thermal event corresponding to the third mass loss is observed in the DSC curve, probably because endothermic and exothermic reactions must be occurring simultaneously and the net heat is not sufficient to produce a thermal event. The total mass loss up to 575 °C is in agreement with the formation of ZnO , as final residue (Calc. = 77.87%; TG = 77.27%).

The gaseous products evolved during the thermal decomposition of the sodium and bivalent transition metal ion mandelates studied in the present work were monitored by FTIR and it has benzaldehyde, CO and CO_2 (Na, Mn, Fe, Co, Cu, Zn) or benzaldehyde, benzoic acid, CO and CO_2 (Ni). The IR spectra of the gaseous products evolved during the thermal decomposition of these compounds are shown in Fig. 5.

4. Conclusion

From TG, complexometry and elemental analysis results, a general formula could be established for the synthesized compounds.

The X-ray powder patterns showed that all the compounds have a crystalline structure, without evidence for formation of isomorphous compounds.

The infrared spectroscopic data suggests that both hydroxyl and carboxyl groups act as coordination sites.

The simultaneous TG–DSC curves provided previously unreported information about the thermal stability and thermal decomposition of these compounds in dynamic air atmosphere.

The monitoring of evolved gases during the heating of mandelic acid showed that the acid decomposes with the release of benzaldehyde, and CO. The thermal decomposition of metal mandelates occurs with release of benzaldehyde, CO and CO_2 for Mn(II), Fe(II), Co(II), Cu(II) and Zn(II) compounds and benzaldehyde, benzoic acid, CO and CO_2 for Ni(II) compound.

Acknowledgements

The authors thank FAPESP, CNPq and CAPES Foundations (Brazil) for financial support.

References

- [1] P.L. Putten, *Antonie Van Leeuwenhoek* 45 (1979) 622–623.
- [2] A. Fischinger, A. Sarapu, A. Companion, *Can. J. Chem.* 47 (1969) 2629–2637.
- [3] P.V. Khadikar, S.D. Chauhan, M.G. Kekre, R.L. Ameria, *Sci. Cult.* 37 (10) (1971) 491–492.
- [4] R. Carballo, B. Covelo, S. Balboa, A. Castiñeiras, J. Niclos, *Z. Anorg. Allg. Chem.* 627 (2001) 948–954.
- [5] A. Beghidja, S. Hallynck, R. Welter, P. Rabu, *Eur. J. Inorg. Chem.* (2005) 662–669.

- [6] S. Balboa, R. Carballo, A. Castiñeiras, J.M. Gonzales-Perez, J. Niclós-Gutiérrez, *Polyhedron* 27 (2008) 2921–2930.
- [7] H.A. Flaschka, *EDTA Titrations: An Introduction to Theory and Practice*, 2nd ed., Pergamon Press, Oxford, 1964.
- [8] C.N. de Oliveira, M. Ionashiro, C.A.F. Graner, *Eclét. Quím.* 10 (1985) 7–10.
- [9] F.J. Caires, L.S. Lima, C.T. Carvalho, M. Ionashiro, *Thermochim. Acta* 500 (2010) 6–12.
- [10] F.J. Caires, L.S. Lima, C.T. Carvalho, R.J. Giagio, M. Ionashiro, *Thermochim. Acta* 497 (2010) 35–40.
- [11] K. Nakamoto, *Infrared and Raman Spectra of Inorganic and Coordination Compounds, Part B*, 5th ed., Wiley, New York, 1997, pp. 58–61.
- [12] L. Biernack, S. Pokrzywnicki, *J. Therm. Anal. Calorim.* 55 (1999) 227–232.
- [13] Z.P. Xu, H.C. Zeng, *J. Mater. Chem.* 8 (11) (1998) 2499–2506.